

Advanced Iso-Grid Fairing Qualification Test For Minotaur Launch Vehicle

Greg Sanford
CSA Engineering
3550 Aberdeen Ave. SE
Kirtland AFB, NM 87117-5776

John E. Higgins and Jeffrey Welsh
Air Force Research Laboratory
Space Vehicles Directorate
3550 Aberdeen Ave. SE
Kirtland AFB, NM 87117-5776

Abstract: The development of the grid-stiffened fairing to be flown on the Minotaur launch vehicle has made significant progress over the past five years. During November and December 2002, this qualification structure was subjected to static qualification testing at the Air Force Research Laboratory (AFRL/VS) at Kirtland Air Force Base. The 6 m (20 ft) tall fairing was constructed of a carbon fiber composite grid structure that was over-wrapped to create a laminated skin. Upon completion of curing and machining, the fairing was cut in half to create the classic “clam-shell” fairing. Metallic joints were bonded and fastened to the fairing at all interfaces to complete the assembly process and simulate attachment of the base to a launch vehicle. Static qualification of the fairing tested the integrity of the fairing, thereby proving the design and manufacturing process. Loads were applied incrementally in a static loading scenario. The applied load envelope exceeded worst-case dynamic flight conditions with an added safety factor of 25%. At peak load the fairing must maintain structural integrity remaining within the defined dynamic displacement envelope.

Load application was accomplished through hydraulic actuators attached to the fairing by two means. Shear (lateral) loads were distributed over a large amount of surface area through the use of wide-body polyester straps. Additional loads were applied to the forward end or nose of the fairing. An aluminum “load head” was bolted in place of the nose cap, with actuators applying load directly to the load head. The fairing and all actuators were bolted to a large steel frame that provided a rigid interface for load reaction. A multi-channel, servo-hydraulic load controller was used to ensure all loads were within predetermined error bands. Additional safety measures were designed into the load control software to prevent overloading and uneven loading of the test article.

Data was collected during the test from a variety of sensors. Traditional displacement transducer and strain gage data were recorded with a 256-channel data acquisition system. In addition, full field displacement was monitored at critically loaded fairing sections and downloaded by means of digital photogrammetry. This system used three high-resolution cameras to record images at various intervals of load application. Post-processing the images gives the analysis team insight into the relative skin and rib displacements in the tapered base of the fairing structure. This paper summarizes the test results, discuss the overall performance of the fairing under the test loads, correlate test response and analysis, as well as identify lessons learned.

KEYWORDS: fairing, spacecraft, testing, iso-grid, and composite

BACKGROUND

Over the past four years the Air Force Research Laboratory has worked with SMC Det 12 at Kirtland AFB, New Mexico; Boeing Phantom Works in Seattle, Washington; and Orbital Sciences in Phoenix, Arizona, to develop manufacturing procedures, design requirements and a comprehensive design basis to produce a new fairing for the Minotaur launch vehicle. During the summer of 2002, the first such composite isogrid fairing design was approved by this team and manufactured in Seattle by Boeing. The fairing was shipped to the AFRL/VS Laboratory at Kirtland AFB, New Mexico, in early November. Two Flight Qualification tests were performed using a load frame and instrumentation system developed by AFRL. This paper discusses the experiment objectives and test setup for these tests, including unique structure response issues for the composite iso-grid design. Results of these tests are summarized and recommendations for further system development are discussed. The overall conclusion drawn from this testing is that the fairing design is structurally sound and suitable for further flight development. The first launch demonstration of the new fairing is scheduled for the summer of 2004. Fabrication of the second fairing, to be used for this launch is currently underway.

EXPERIMENT OBJECTIVES

Design requirements for this fairing and static qualification test loads were developed by the launch contractor for Minotaur missions, Orbital Sciences (OSC). OSC developed a static load criteria requiring four lateral loads and one axial load to be applied proportionally at all times and rising to peak values exceeding calculated flight loads (shear, bending and axial section loads) at all elevations. The lateral loads were to be applied along two separate azimuths in the two test cases. For the first test the lateral loads were applied normal to the plane formed by the separation rails of fairing. The second test applied these loads through the plane of the separation rails. The Qualification Fairing design included numerous standards and representative door panels. One of the larger such doors (a battery access hatch) was located at a point of maximum shear, axial, and bending loads for the first test. The potential for buckling or skin to rib joint failure was considered to be greatest for this test configuration. The second test was oriented such that the aluminum separation rails and thick composite connection pad-ups for these rails were resisting overall bending and represented lower potential risk to the structure.

The major objectives of these two tests were as follows:

- A. To observe and confirm that the structure could resist the applied loads without permanent distress or damage.
- B. To measure representative strain levels for the applied loads to confirm the nature of the structure response.
- C. To measure overall structure displacement under the applied loads to confirm calculated structure stiffness. This measurement is essential to confirm the required flight dynamic displacement envelope is not violated, thereby preventing the fairing and flight payloads from coming into contact.

Secondary objectives of these test included the following:

- A. Provide supplemental instrumentation to insure that intended loads and restraint conditions were met.
- B. Assess the nature of unique skin buckling response of the isogrid structure throughout the applied load range at likely regions of distress.

TEST CONFIGURATION

The Minotaur Fairing Qualification tests were conducted in a general-purpose steel frame load fixture. The test fixture was used previously to flight qualify two separate payload adapter structures (EELV Secondary Payload Adapter (ESPA) for the EELV launch vehicle and a Multiple Payload Adapter (MPA) unit for the Minotaur launch vehicle). To suit the dimensions of the Minotaur fairing, the top cross bracing of the fixture was temporarily removed and an additional twelve feet of vertical column members were inserted at the four vertical uprights of Figure 1. The three lower lateral loads were applied by actuators to belts that were draped into position and gravity offloaded as needed to insure correct angle of load application. These belts distributed load to the fairing through 2 cm thick felt padding on the inside face of the belts. Aluminum spreader bars were provided to prevent contact of belt to fairing on the unloaded face of the fairing. Load angle was confirmed by multiple measurements with a digital inclinometer at 10, 20, 30 and 40 percent of design load. Typical frame to actuator connections and actuator to belt/nose plate connections are illustrated in Figure 2.

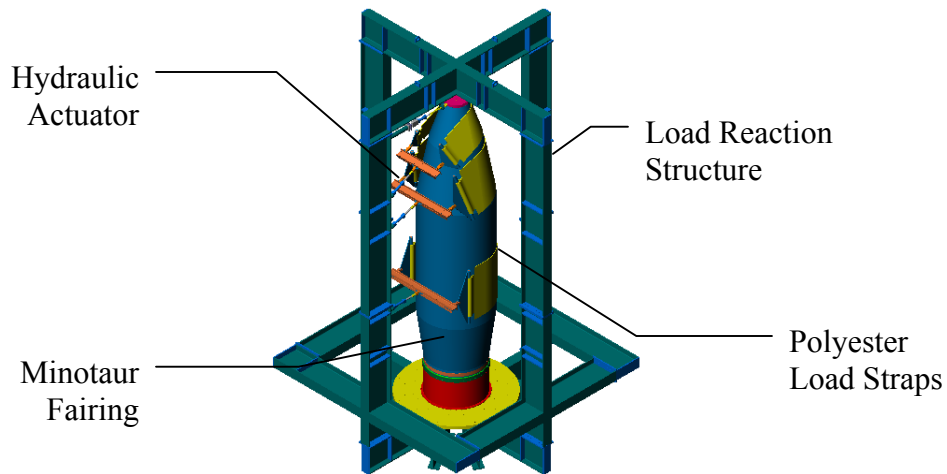


Figure 1. Test Configuration



Figure 2. Typical Actuator Connections

The largest load in each test was applied axially through a strap extending through the interior of the fairing and pulling downward. The nose cone for the fairing was replaced in these tests with a thick aluminum plate (see Figure 3). The plate rested on a circumferential rib supported by numerous vertical ribs at the nose. This plate was loaded by an internal belt from below and a fourth (upper) actuator laterally.



Figure 3. Aluminum Nose Plate Test Fixture

The load frame supported the fairing from below on a 3-meter diameter, 10 cm thick steel plate resting on steel I beams along 12 azimuths. A cylindrical steel structure containing a man-access port was bolted to the steel plate, a flexible aluminum ring consistent with the normal fairing attachment system for the Minotaur launch vehicle was bolted between the steel cylinder and the base of the composite fairing (see Figure 4). The access port in the steel cylinder was used to service the largest actuator loading the internal belt and to port all internal strain gage cables.

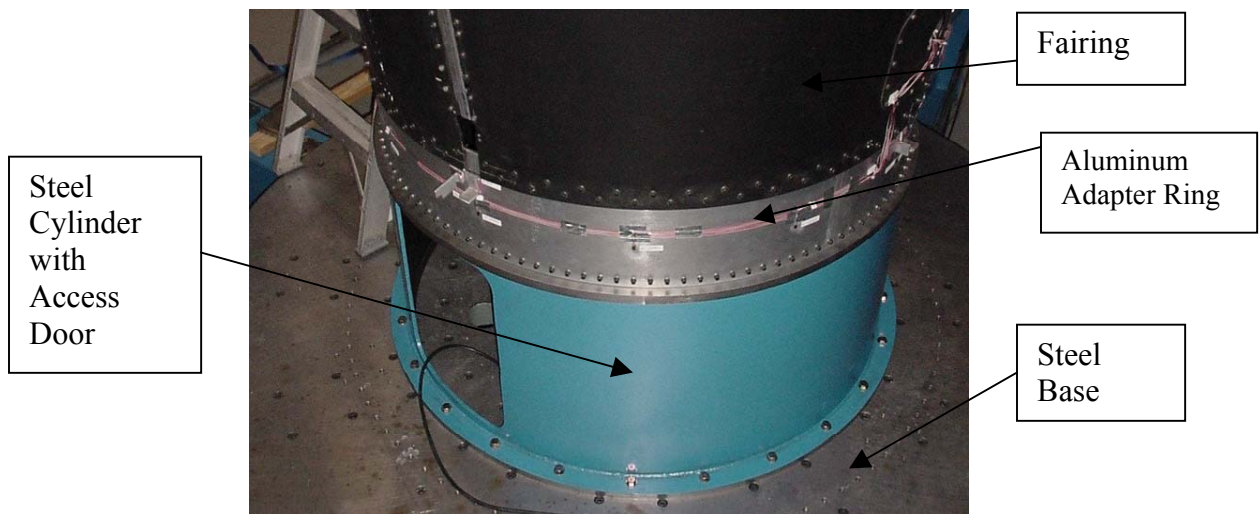


Figure 4. Support structure and aluminum interface

The following nominal peak static loads and orientations were to be applied for each load case at the Qualification loads equal to 125 percent of the design (or flight) load:

Table 1. Applied Static Loads

Load Description	Peak Force (kg)	Orientation from Horizontal (deg)
Internal belt	8965	90
Lateral nose plate actuator	934	0
Upper external belt	2164	26.3
Middle external belt	3606	16.2
Lower external belt	1874	0

In both tests, the upper and middle belts varied by less than one degree from the prescribed values. The angle was adjusted to be at least as great as the prescribed value, and the lateral nose plate actuator loads were increased slightly as needed to insure the correct bending moment at the base of the fairing.

ACTIVE INSTRUMENTATION, PHOTOGRAMMETRY, AND PHOTO/VIDEO DOCUMENTATION

Each load test provided for 70 channels of strain data located inside the fairing. These strain gages were a mixture of axial strain gage pairs placed at mid-height of helical and axial ribs between intersecting rib nodes and three gage Rosettes placed at central locations between nodes on the skin of the structure. As illustrated in Figure 4, this strain instrumentation was generally located in the lower half of the fairing at locations of maximum overall loading, at points of possible localized strain peaking near door openings, and at points requiring minor post manufacturing repairs.

Additionally, 12 axial strain gages were placed in vertical orientations at 30-degree increments around the exterior of the aluminum base ring. The gages were placed at mid elevation on the ring (see Figure 5) in an attempt to confirm overall axial and bending moments on the structure, thereby treating the aluminum ring as a large load-cell structure. Although this treatment was well recommended from prior sandwich panel fairing designs tested by Boeing, the distribution of rib loads to the base pad-ups in the Minotaur Iso-grid structure resulted in some unanticipated local peaking. The general trend of bending moment application and axial loading could be assessed from these gages.

Each load test provided for 11 LVDT channels to monitor displacements at the base and nose of the fairing. At the base, axial and circumferential motions were measured at 0, 90, 180 and 270-degree azimuths from the direction of lateral load application. At the nose, circumferential displacements were measured at 90 and 270-degree azimuths from the direction of load application. Additionally one gage at 90-degree azimuth from the direction of load measured radial nose displacement. The sensors were supported from a Unistrut structure supported from the concrete floor of the laboratory and unattached to the load frame (see Figures 5 and 6).

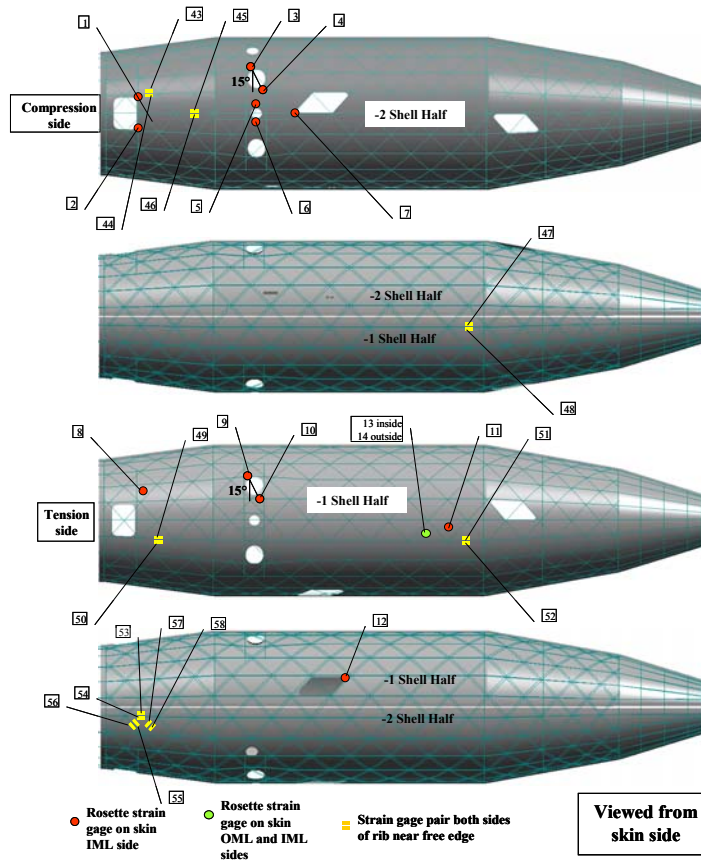


Figure 4. Strain Gage Locations with Reference to Load Case 1



Figure 5. Unistrut LVDT Support Structure

Displacement sensor structure

Typical Displacement sensor

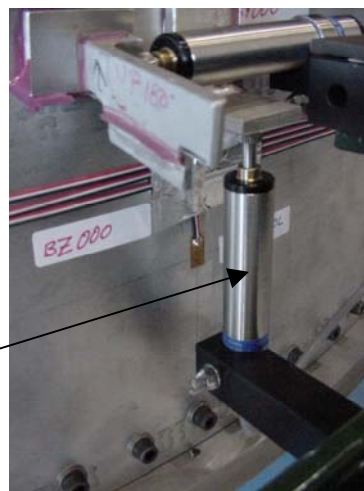


Figure 6. Typical LVDT Installation

During the development and structural component testing of this isogrid design, it was determined that early skin buckling would develop at locations between supporting ribs. From both analysis and test this buckling was found to be harmless to the overall buckling response of the structure, but the curvature at the skin to rib interface resulting from this buckling induced a high peeling stress which could encourage failure at this joint. The joint is formed by polymer bonding only with no fiber penetrating the joint. The high peeling stresses at the joints were controlled by limiting curvature at this interface using larger skin thickness at the lower elevations of the fairing. A photogrammetry technique as described by NASA (Ref 1) was used to measure and confirm the reduction in curvature at the critically loaded lower conic section above the battery door in the first load test.

Three high-resolution digital cameras were located to capture a field of retro-reflective circular targets illuminated by the integral flash of each Olympus Camedia E-20 camera (see Figure 7). The target size and camera ranges were adjusted to provide effective sub-pixel target locations using PhotoModeler 4.0 software. The target locations provided by this software were used to assess radial motions of targets located over ribs and on the skin between ribs.

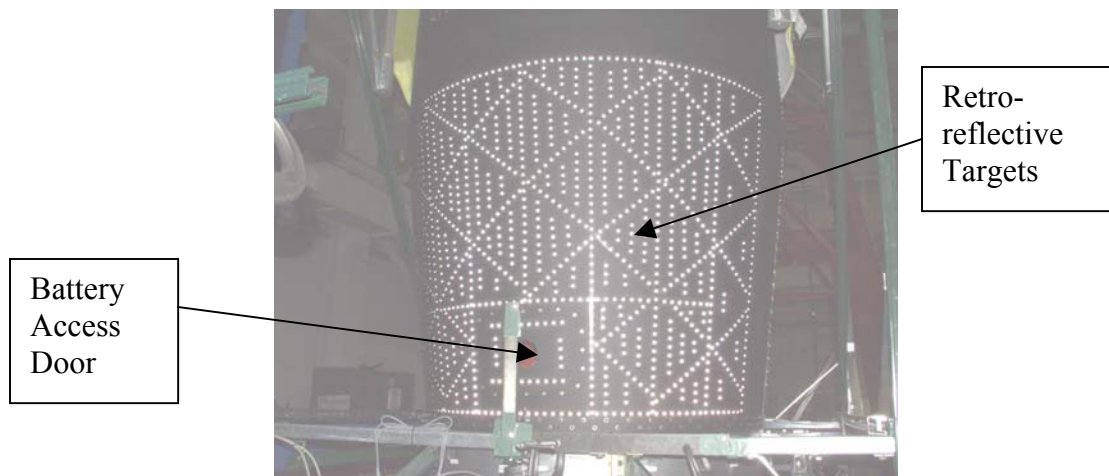


Figure 7. Retro-reflective Targets in Test 1 at Base of Fairing

During the course of each test continuous internal video was recorded for the final run up to peak load with close-up documentation of internal rib deformations in regions of large skin deformations during the initial testing to design load. Digital photos also documented these areas of visible skin buckling and other visible areas of concern during testing.

RESULTS

In reviewing the strain data for these tests, Figures 8 and 9 are quite typical of the type of linear response observed. These gage pairs were located on the most highly loaded compression ribs near the base of the structure. Very little bending is observed. The peak strain levels in Test 2 are about 40 percent low despite being position lower on the structure than the similar Test 1 gage. This reduced strain probably results from the compression plane alignment of the aluminum separation rail adjacent to this Test 2 gage and the thick composite pad-up at the rail to fairing connection.

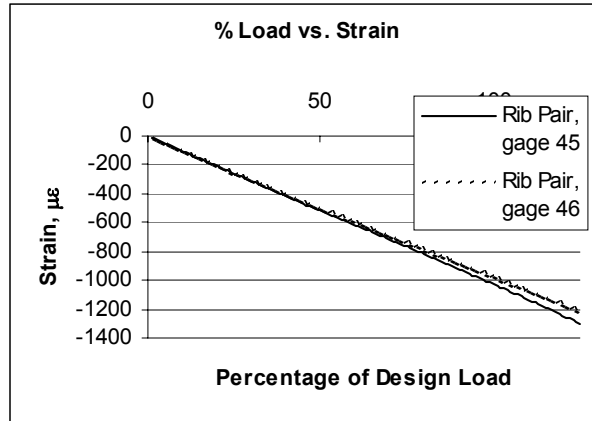


Figure 8. Compression Rib Strain at Fairing Base—Test 1

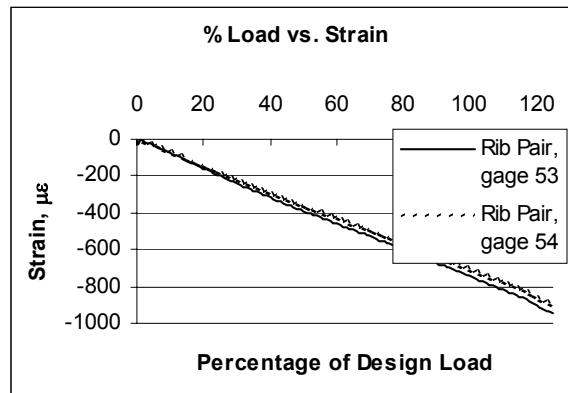


Figure 9. Compression Rib Strain at Fairing Base—Test 2

In Figure 10 the idealized strain gage readings for the aluminum support ring below the fairing base are compared to actual readings for both tests. Strain trends match predictions rather well despite the influence of axial rib peaking, probable bending about the circumferential orientations at the fairing to ring joint, etc. These results suggest good correlation between anticipated and actual load and response at the base of the structure.

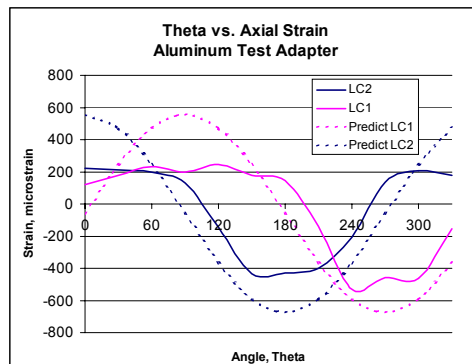


Figure 10. Comparison of Predicted and Actual Strains at the Base Adapter

Predicted lateral deflections at the nose of the fairing were 2.69 cm (1.09”) and 2.31 cm (.91”) for Tests 1 and 2 respectively. As seen in Table 2, the actual displacements were about 40% to 60% greater than anticipated. In the Test 2 orientation, the added bending stiffness provided by the separation rails tended to reduce maximum displacements. Comparing axial LVDT measurements taken at the base of the fairing and noting a relatively large bolted joint slip in aluminum ring connection at the base of the fairing (see Figure 11), a determination was made that the lateral stiffness of the fairing was well within allowable tolerances. Also, no more than .013cm (.005”) of lateral nose displacement was seen in either test, suggesting good balance and minimal torque in the applied loads.

Table 2. Fairing Lateral Displacements
(LVDT 1 & 2 along Plane of Loading and LVDT 3 Normal to Loading)

		LVDT 1	LVDT 2	LVDT 3
		mm	mm	mm
Load Case #1	Initial Reading	0.0	0.0	0.0
	125% Reading	41.6	41.5	1.0
	Final Reading	1.5	1.5	0.0
Load Case #2	Initial Reading	0.2	0.2	0.0
	125% Reading	36.3	36.4	0.0
	Final Reading	1.4	1.6	0.0

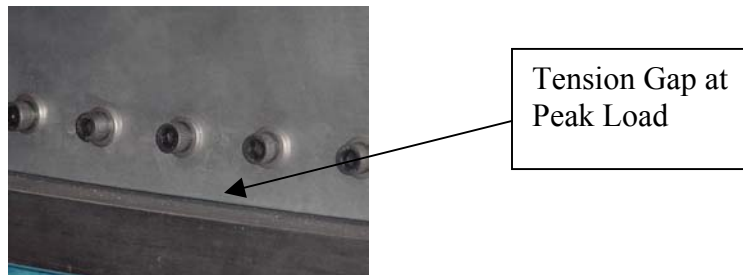


Figure 11. Bolted Joint Slippage at the Base of the Aluminum Ring

The three dimensional model of retro-reflective target locations for Test 1 were compared for the initial (zero) load state and for the peak load state (125% of design). Figure 12 illustrates the local buckling in the skin at the base of the fairing at the peak load. The radial displacements from adjacent ribs to buckled skin node are roughly 1.3 mm (.05”) max and are localized in the pockets of skin between the ribs. These buckles were not apparent to the eye during the test and do not appear to have influenced the primary response of the structure. Visible buckling was only observed at the middle level of the fairing on the compression side.

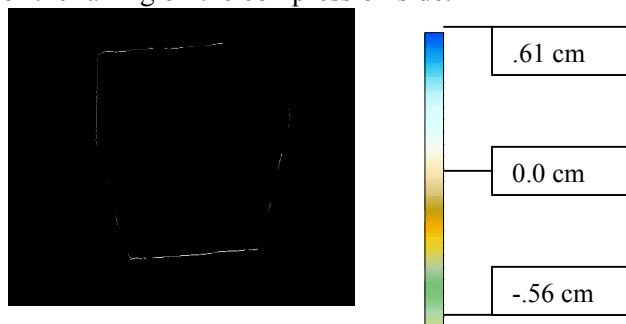


Figure 12. Radial Displacement Field at Compression Side Base of the Fairing in Test 1

SUMMARY

All of the major objectives of these two tests were satisfied. The fairing exhibited no distress of any kind, except for some minor popping noises at lower load level, which were attributed to slippage of bolted joints. Strain response was typically linear and within predicted values for both tests. Overall lateral displacement was within the allowable design criteria and very close to predicted values after giving consideration to unanticipated joint slippage at the base of the fairing.

Indications from displacement gages at the base and nose of the fairing agreed with available load cell data that proper loads were applied and anticipated responses were obtained from the structure. There is no significant indication of asymmetric loading or response.

The peak skin buckling response in this structure did not occur at the base of the fairing as anticipated. The skin thickness was varied with elevation in the fairing to maintain a somewhat balanced strain response. The point of greatest radial skin displacement localization was missed; however, the available photogrammetry data clearly demonstrates that skin buckling is present at the higher loads, even though not visibly apparent to the eye. Neither the load level skin buckling measured at the base of the fairing or the more visible (.2 to .5 cm) skin buckling observed at mid-heights of the fairing seemed to impact the linear response of the primary load-carrying iso-grid.

REFERENCES

1. AIAA 2002-1332: POST-BUCKLING TEST RESPONSE AND ANALYSIS OF FIBER COMPOSITE GRID-STIFFENED STRUCTURES, John E. Higgins, Peter M. Wegner, Barry Van West, Adrian Viisoreanu.
2. AIAA 2002-1733: INSTRUMENTATION AND EMPIRICAL ASSESSMENT OF POST-BUCKLING RESPONSE IN GRID-STIFFENED STRUCTURES, Barry P. Van West, Charles D. Capps, Mitchell D. Voth, Jonathan M. Saint Clair.
3. NASA/TM-2002-211739: PHOTOGRAMMETRY METHODOLOGY DEVELOPMENT FOR GOSSAMER SPACECRAFT STRUCTURES, Richard S. Pappa, Jonathan T. Black, Alan Walford, Stuart Robson, Mark R. Shortis